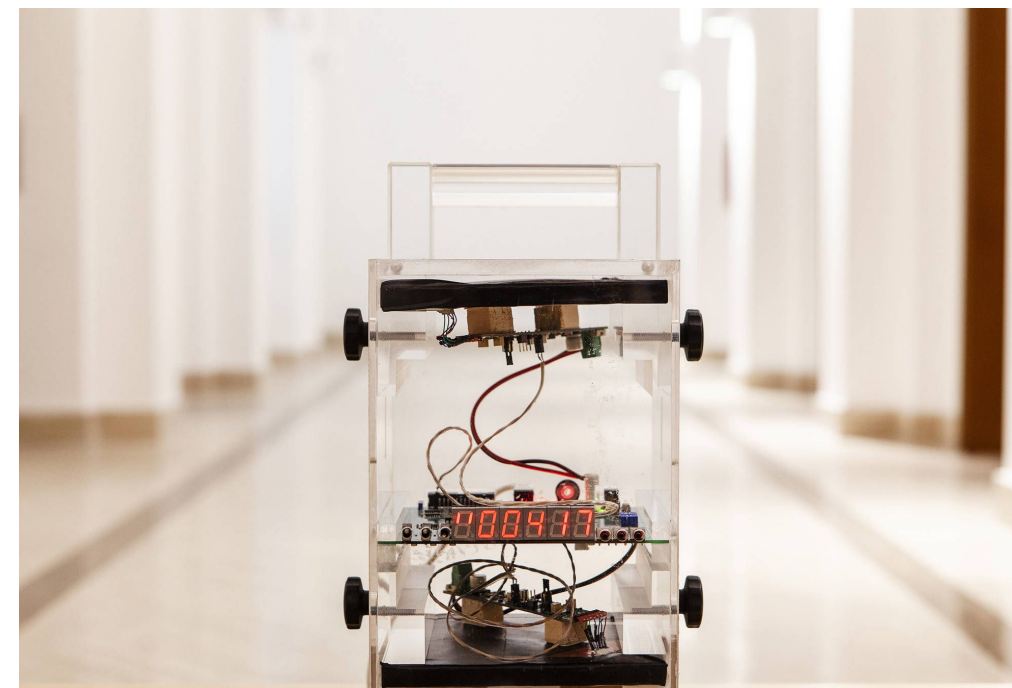




LICEO SCIENTIFICO STATALE
ARCANGELO SCACCHI

COSMIC BOX



May 27th 2026



**Seeing Inside Structures with Cosmic Rays:
A Non-Invasive Approach
(Preliminary results)**

Relatori: Dafne Abrescia (3A), Michele Valentini(4C), Giuseppe Valerio (3I)





The floor below street level of our school harbours an ex anti-aircraft bunker. The topographic mapping made through field surveys will be object of an activity carried out by the students of the historical-architectural course of our school.





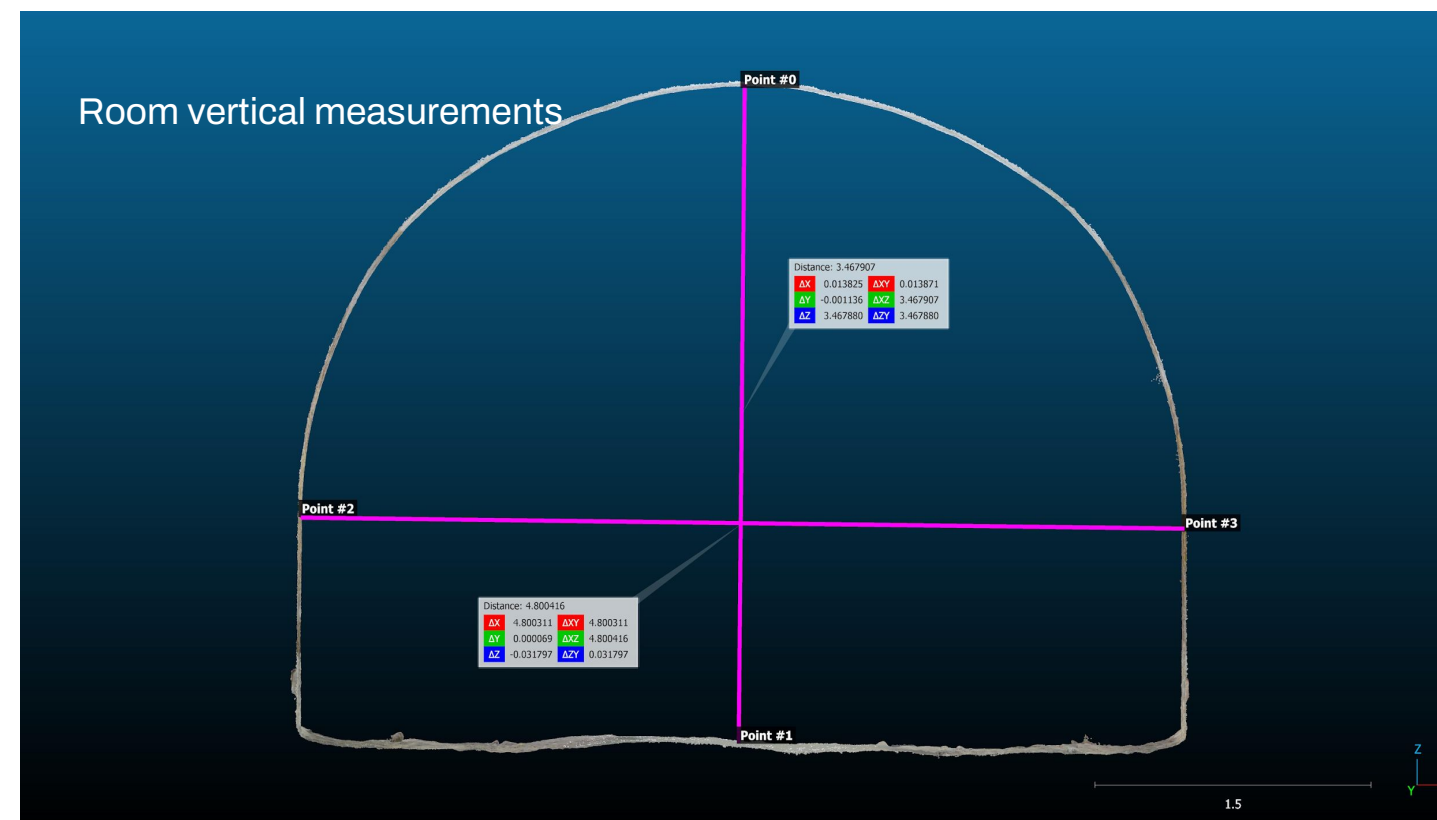
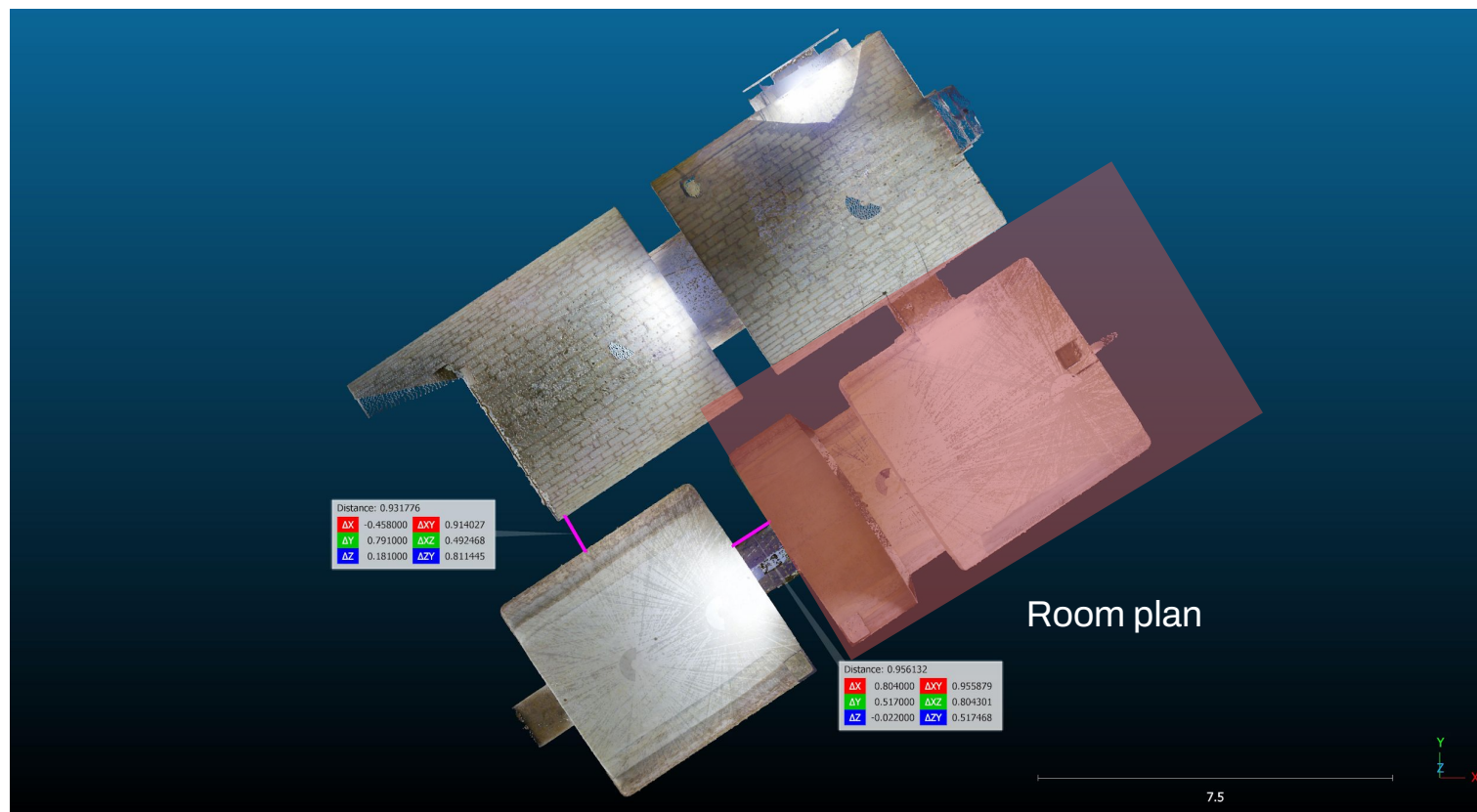
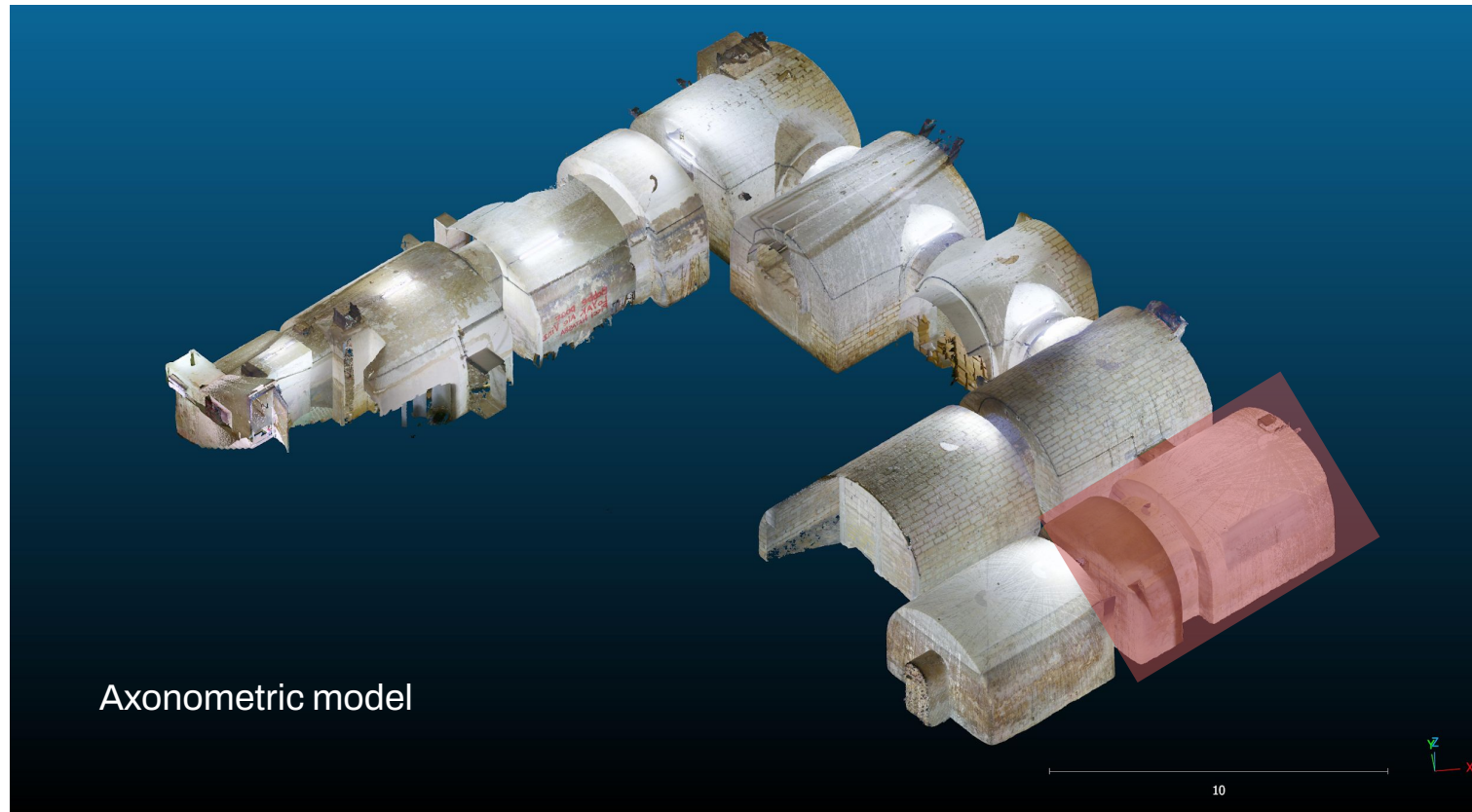
Site context & Goals

- **Historical Background:** The bunker was originally part of the 19th-century residence of Prosper Chartroux, built in 1882.
- **Original Function:** Initially designed for large-scale olive oil storage, a common architectural feature in historical residences of Bari
- **WWII Adaption:** During the Second World War, these vaulted cellars were repurposed as air-raid shelters

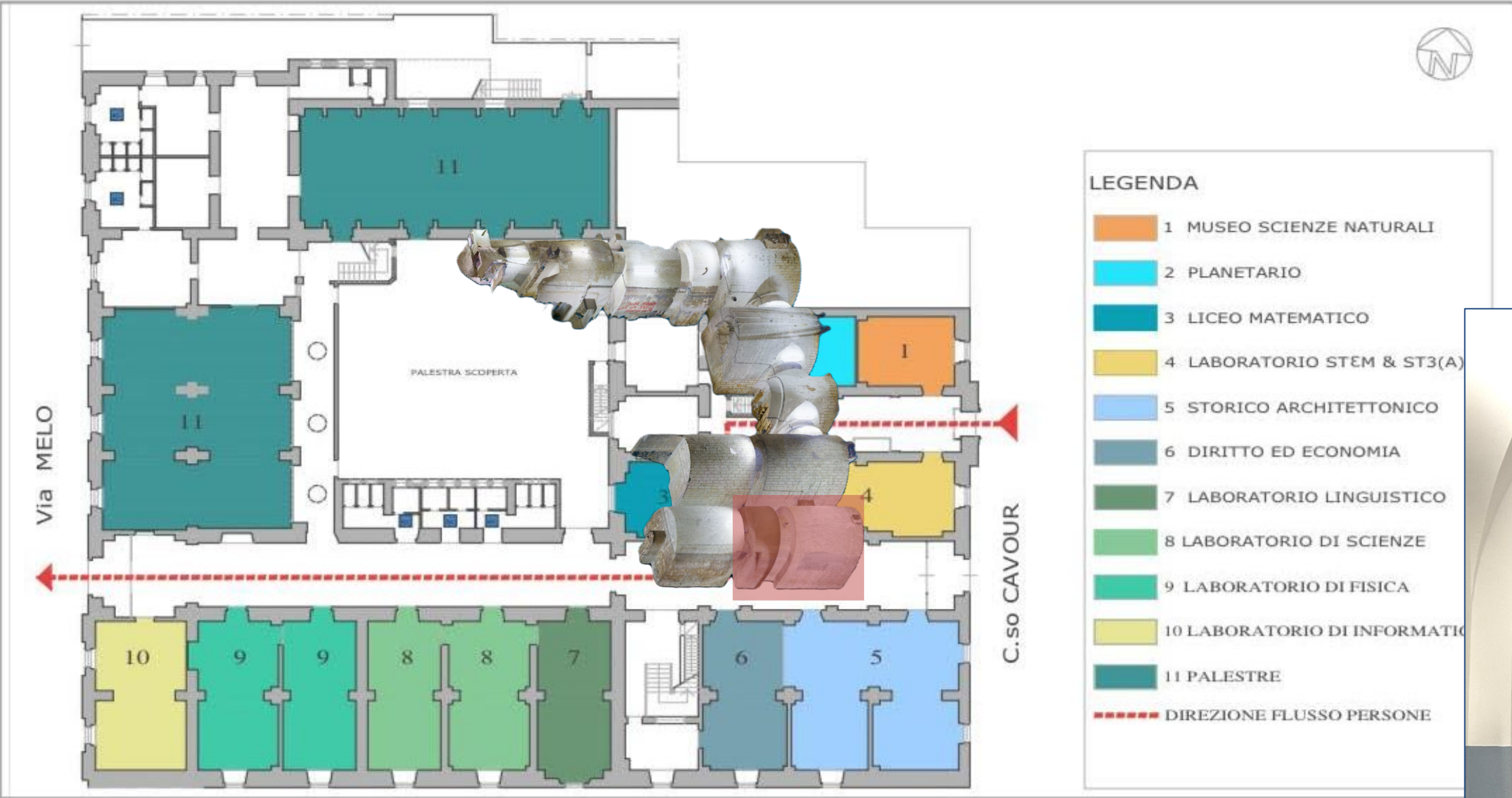


- **Project Aim:** Mapping the structural thickness of the bunker's final chamber using muon flux attenuation, with a specific focus on the arched vault where structural thickness varies significantly due to its geometry.

Geometric Survey: Laser Scanner

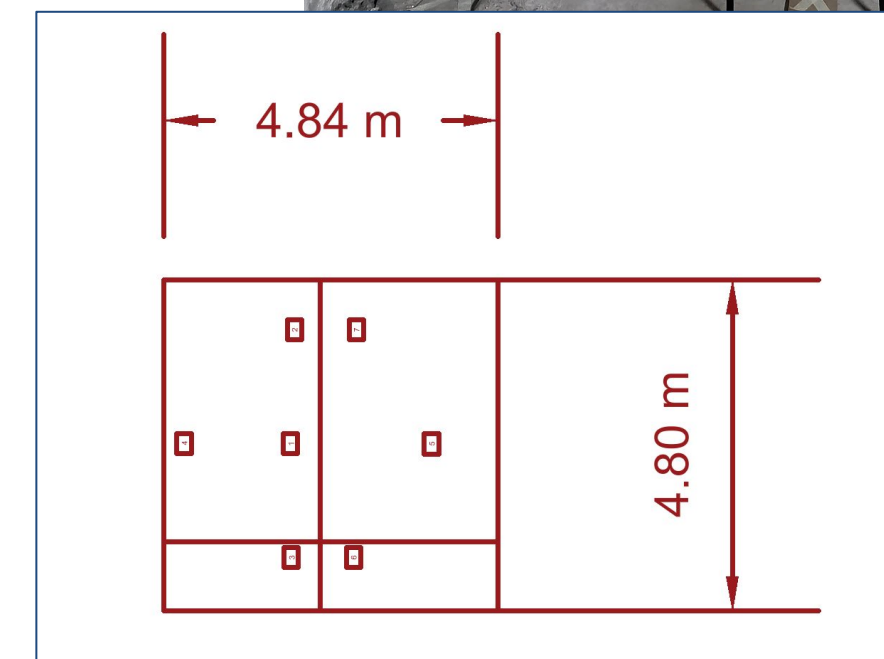
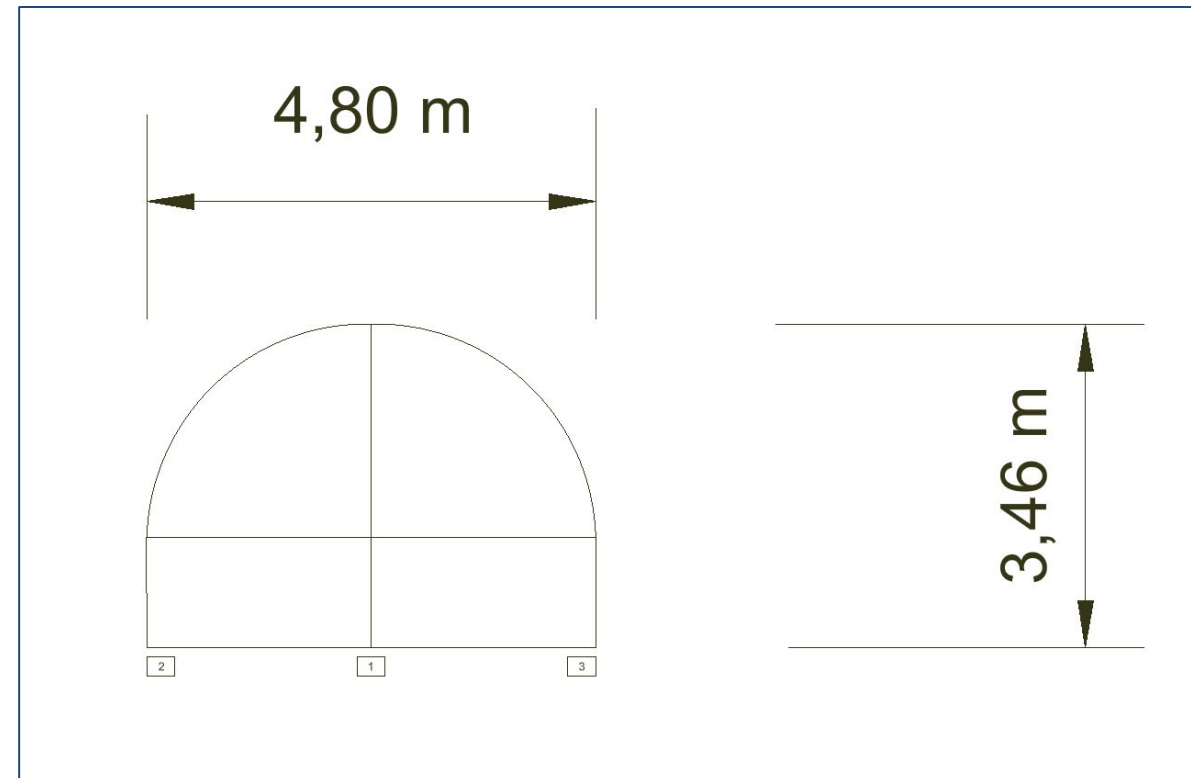
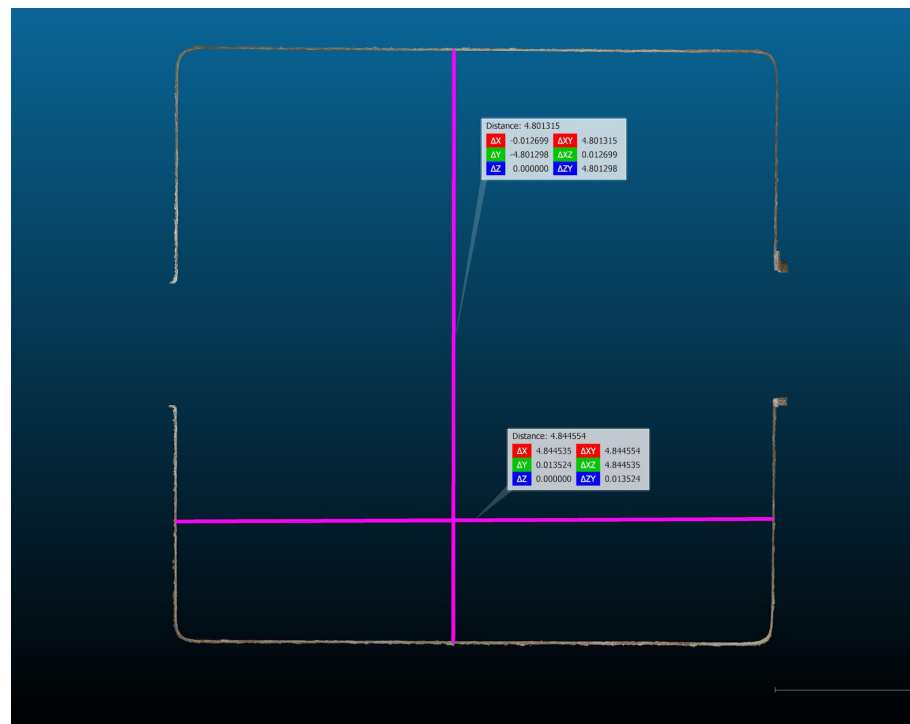


Ground floor plans

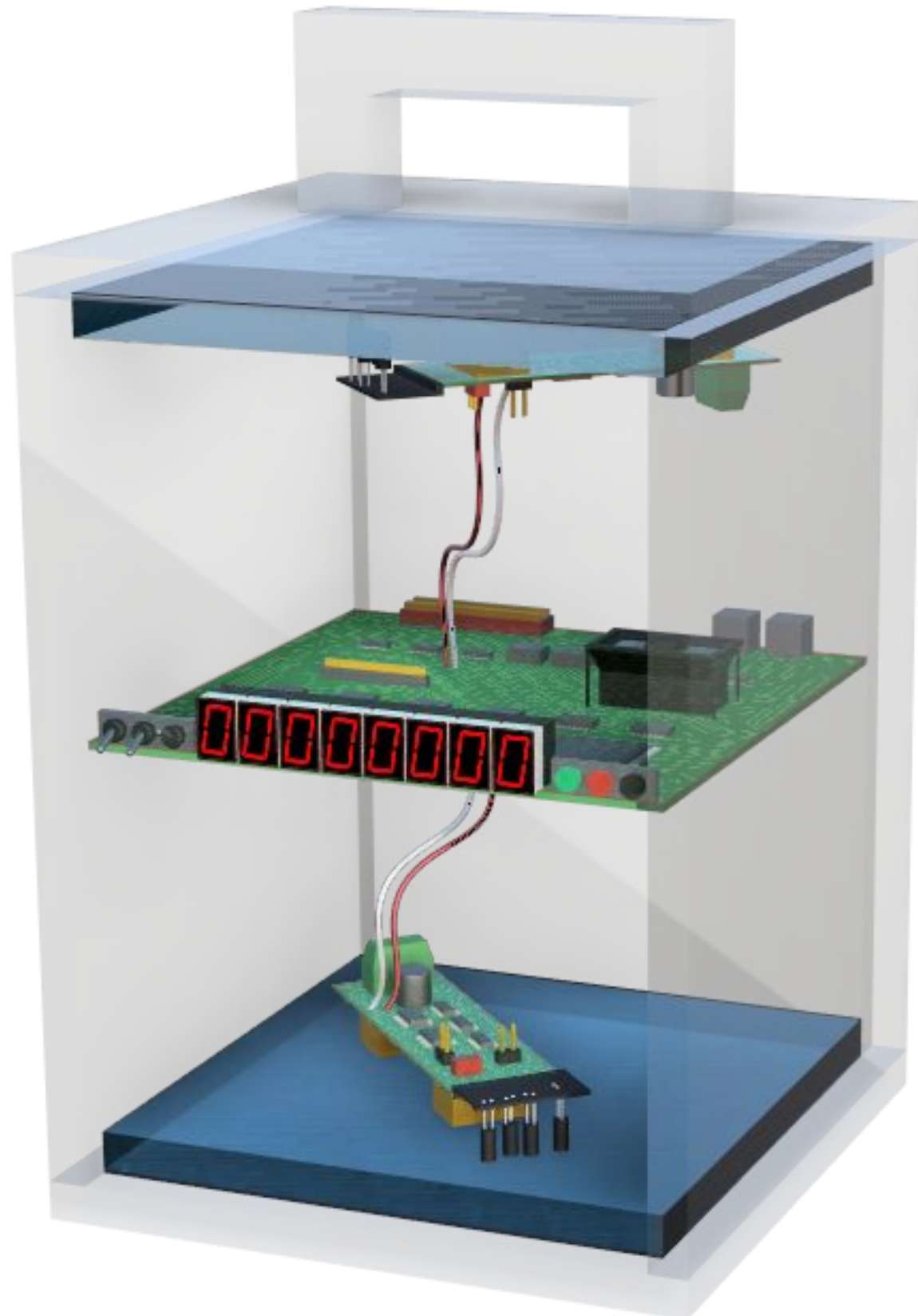


Geometric Survey: Laser Scanner

- **Room dimension:** An almost perfectly square environment measuring 4.80m x 4,84 m
- **Maximum Height (H):** The central axis of the barrel vault is located 3.46 m above the floor.
- **Lateral Thickness:** The internal load-bearing walls separating the rooms are approximately 0.95 m thick.



Detector: Cosmic Box



Scintillation Tehnology

Plastic scintillators (15x15x1cm) coupled with SiPMs for coincidence-based muon detection. The distance between the scintillation planes is approximately 27 cm, resulting in an angular acceptance of $\sim 40^\circ$.

Environmental Monitoring

Sensors monitor pressure, temperature and humidity during data acquisition to ensure stability.

Acceptance

The distance between the 2 scintillator plates determine the minimum angle θ that the trajectory of a muon must have in order to be recorded by both plates: if the trajectory had a bigger angle, the passing of the muon would be detected as a noise

Therefore, considering the CB we used had:

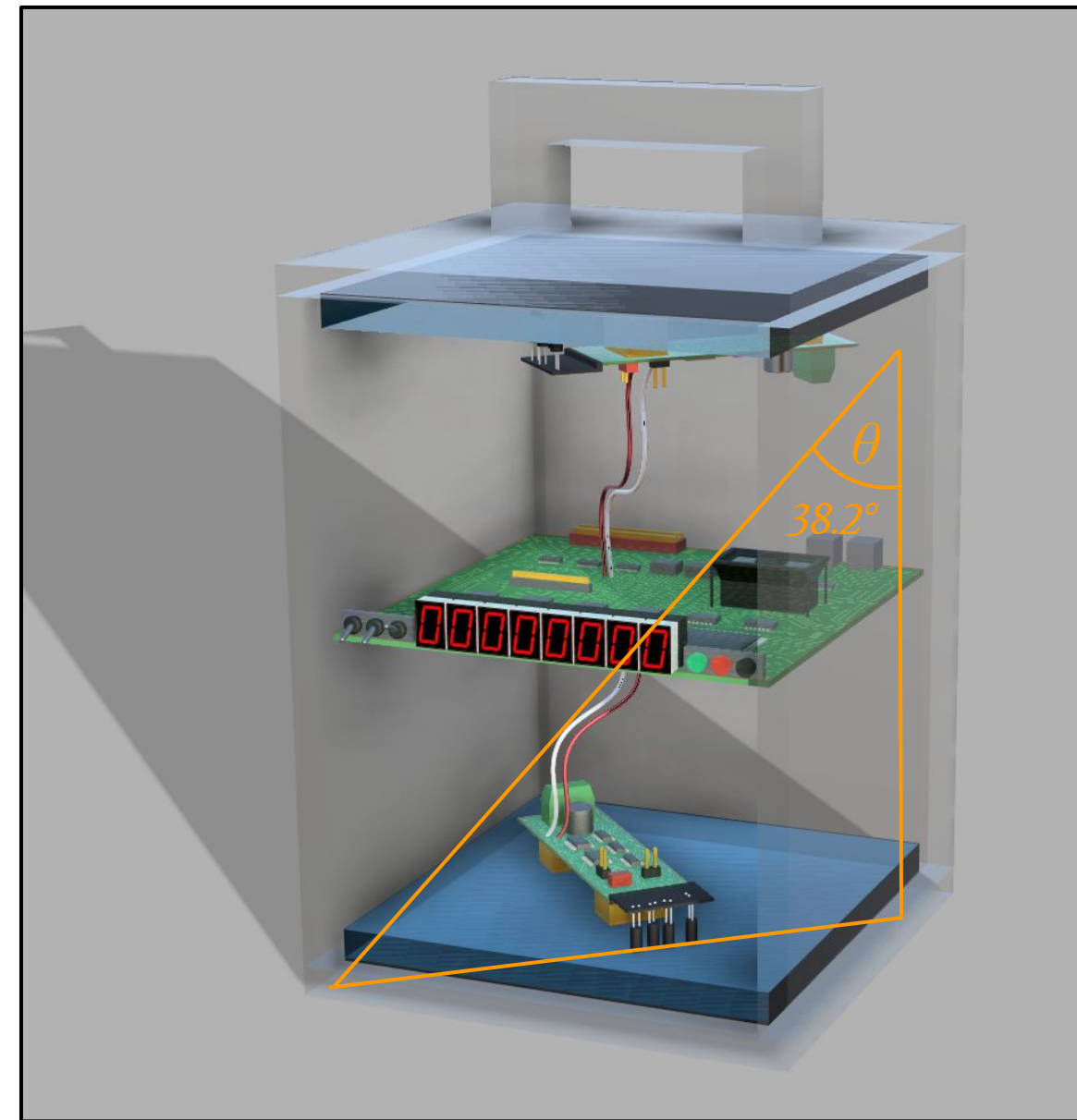
$$h = 27 \text{ cm}$$

$$d = 21.2 \text{ cm}$$

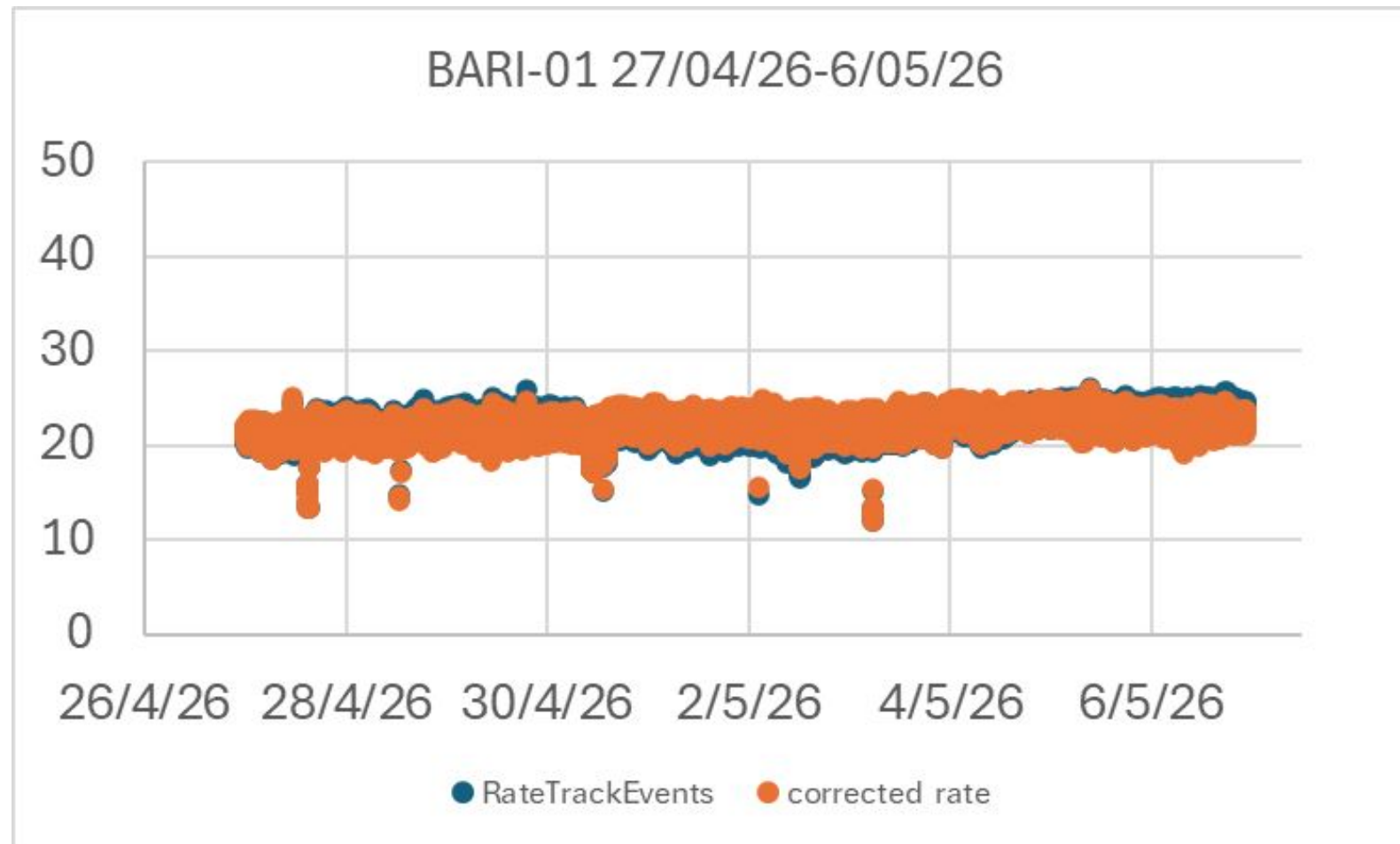
$$\sin\theta = 0.604$$

$$\sin\theta = \frac{d}{\sqrt{h^2 + d^2}}$$

$$\theta = 38.2^\circ$$

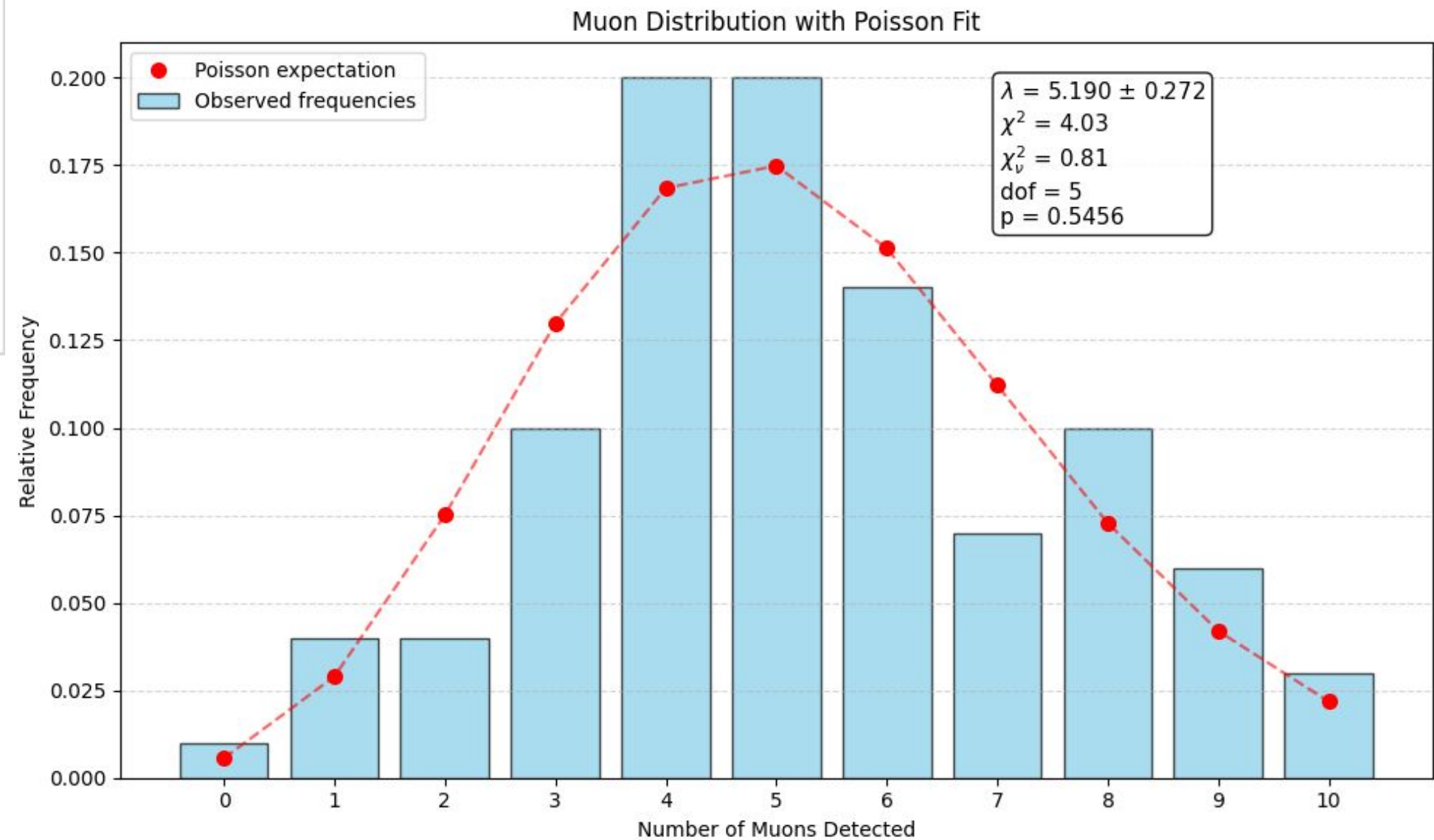


Cosmic box calibration at the ground floor



BARI-01 data from
27/04/2026 to 06/05/2026.

No significant variation of
the rate have been found



Poisson Distribution

Poisson distribution is used as a model to have the number of times an event occurs in an interval of time .

The distribution is based on the following assumptions:

- the events are random and rare ;
- an event is described by integers;
- the average rate at which events occur is independent of any occurrences.

Given an average value λ , the probability of x events taking place is given by the function:

$$f(x, \lambda) = P(X = x) = \frac{\lambda^x \cdot e^{-\lambda}}{x!}$$

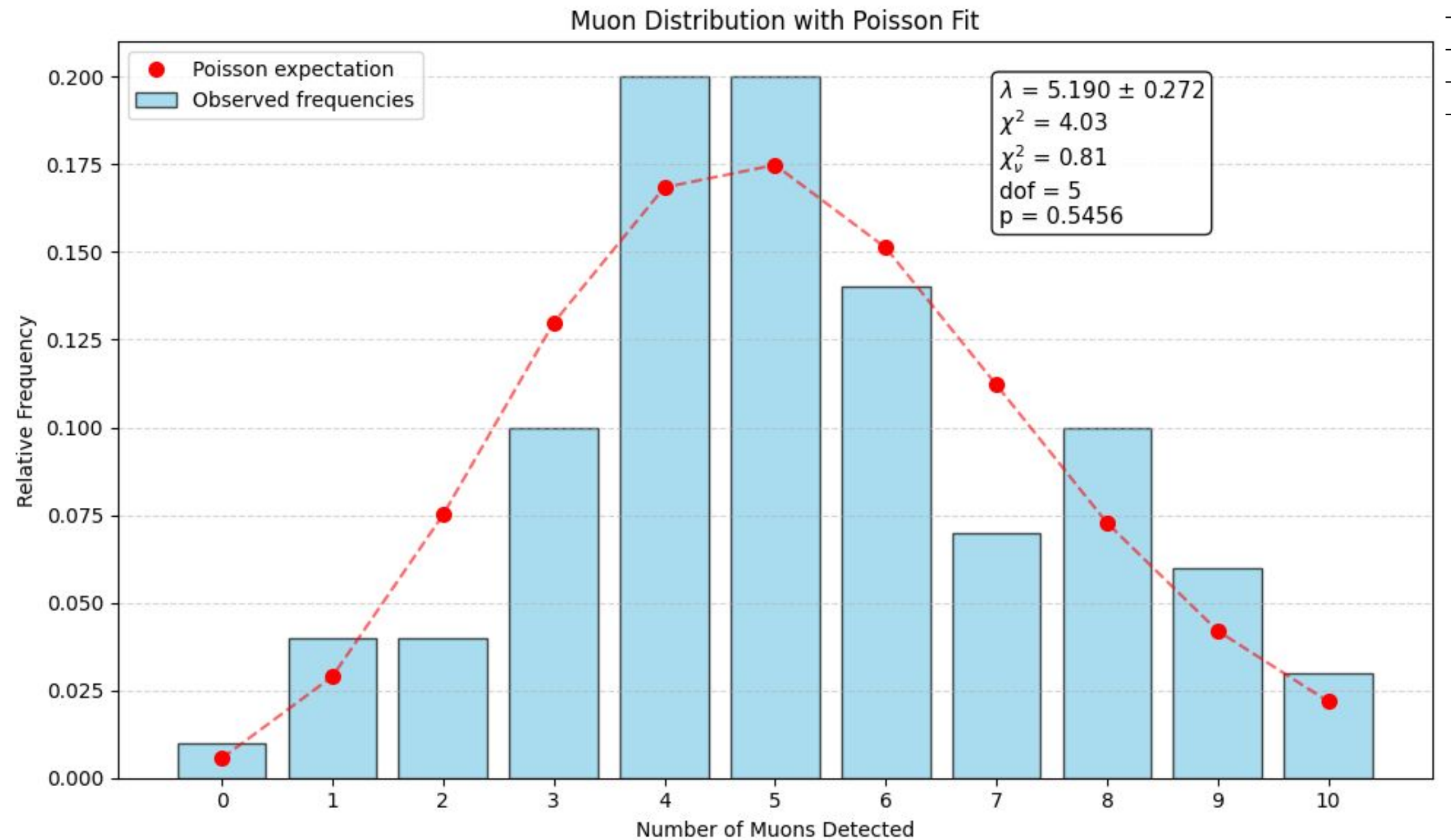
Poisson Distribution @ ground floor

To compare the histogram obtained with the experimental data with that predicted by the Poisson distribution, the weighted average of all measures was calculated:

$$\lambda = \frac{\sum(x_i \cdot p_i)}{\sum p_i}$$

where, λ is the weighted average of the number of measurements according to the experimental frequency and x is the number of measurements.

count number	Number of mesuraaments	experimental frequency	teoric frequency
0	1	0,01	0,01
1	3	0,04	0,03
2	3	0,04	0,08
3	7	0,10	0,13
4	14	0,20	0,17
5	14	0,20	0,17
6	10	0,14	0,15

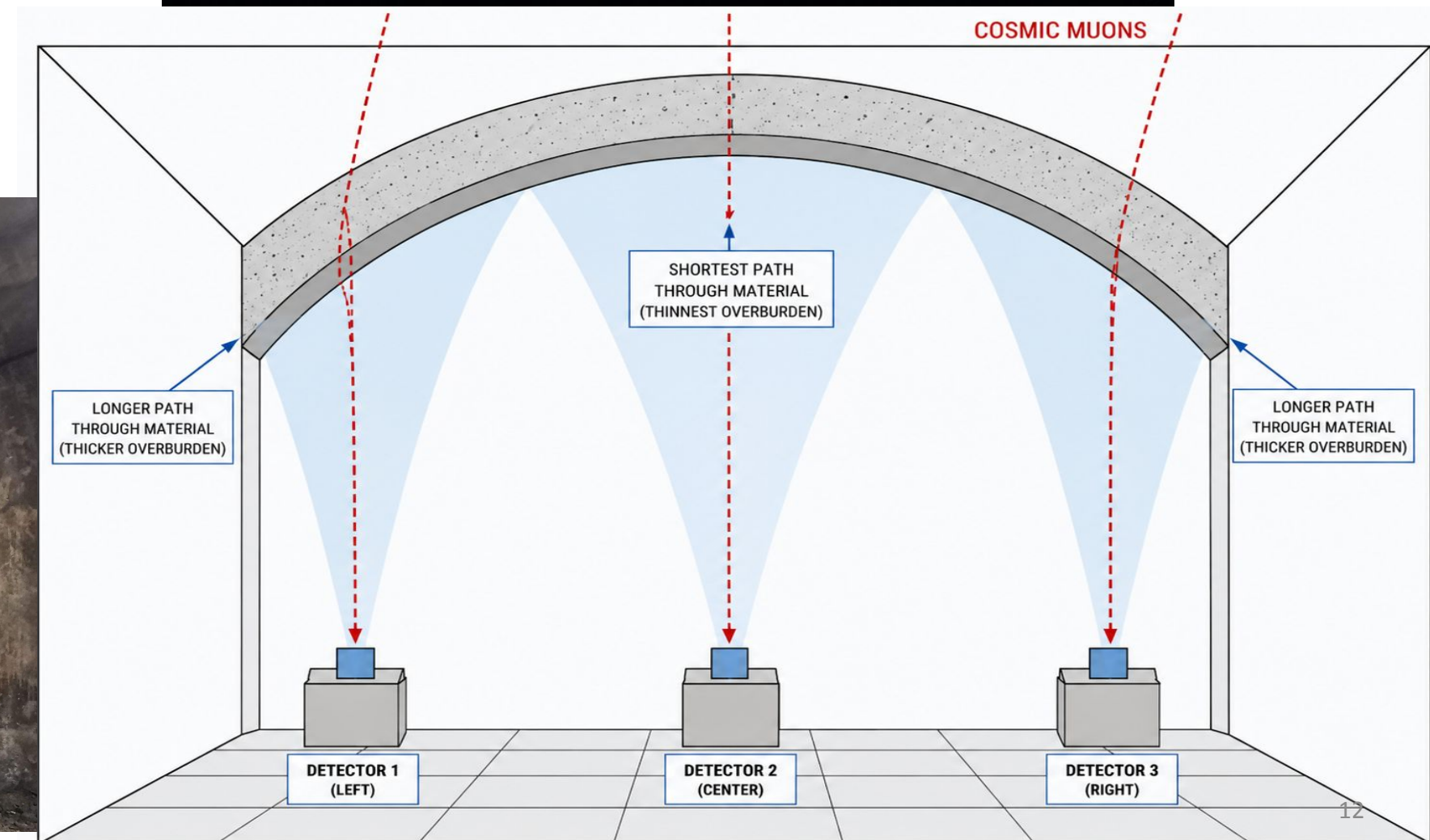
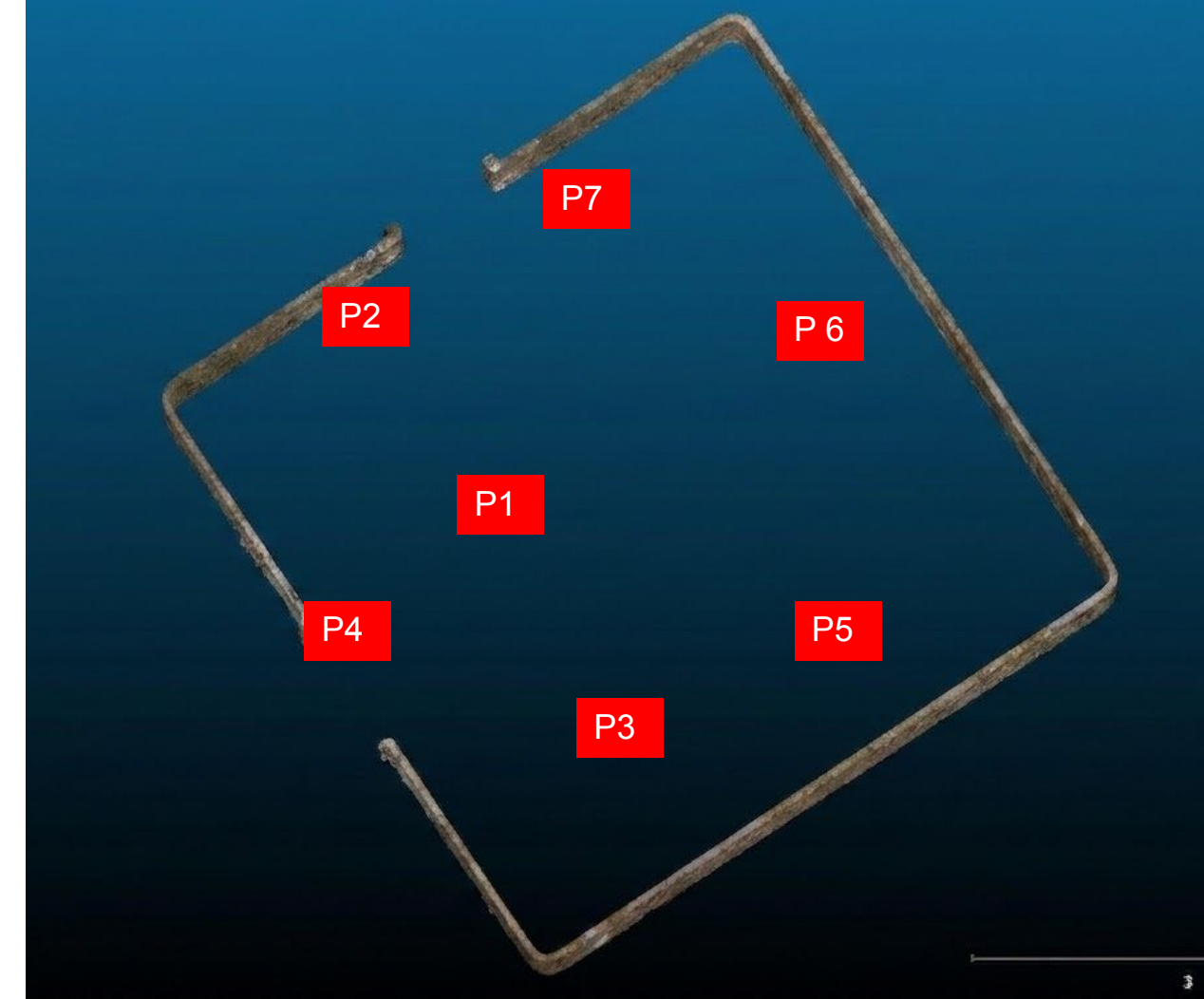


****This analysis is based on data collected from the ground floor with $\lambda=5.19 \pm 0.27$***

Measurement protocol

- **Calibration:** at the ground floor
- **Data Acquisition**

All the measurements were taken in the bunker every **ten minutes** at three specific points under the arch and at the corresponding reference points on the upper floor as well. Together with the three points in the bunker we made other measurements in four other locations in the room of the bunker.



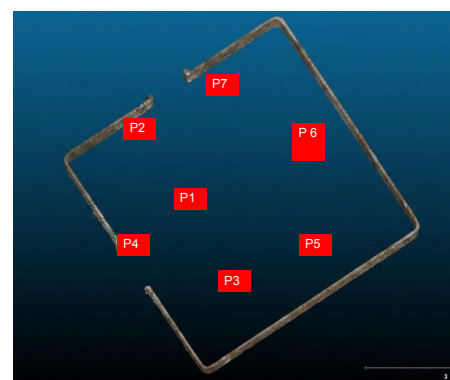
Raw Data: Muon Counts Bunker

p=1016.5 hPa

T= 19.9°C

Humidity 71%

Location	Slot 1 (600s)	Slot 2 (600s)	Slot 3 (600s)	Average values	Total counts
P1 (Arch center)	43	51	44	46	138±11.7
P2 (Right Side)	40	30	32	34	102±10.1
P3 (Left Side)	35	36	40	37	111±10.5
P4	43	44	42	43	129±11.4
P5	46	43	44	44	133±11.5
P6	47	42	47	45	136±11.7
P7	32	34	38	35	104±10.2



We aggregate the total counts to calculate the intrinsic statistical error
the relative error.

$$\sigma = \sqrt{N}$$

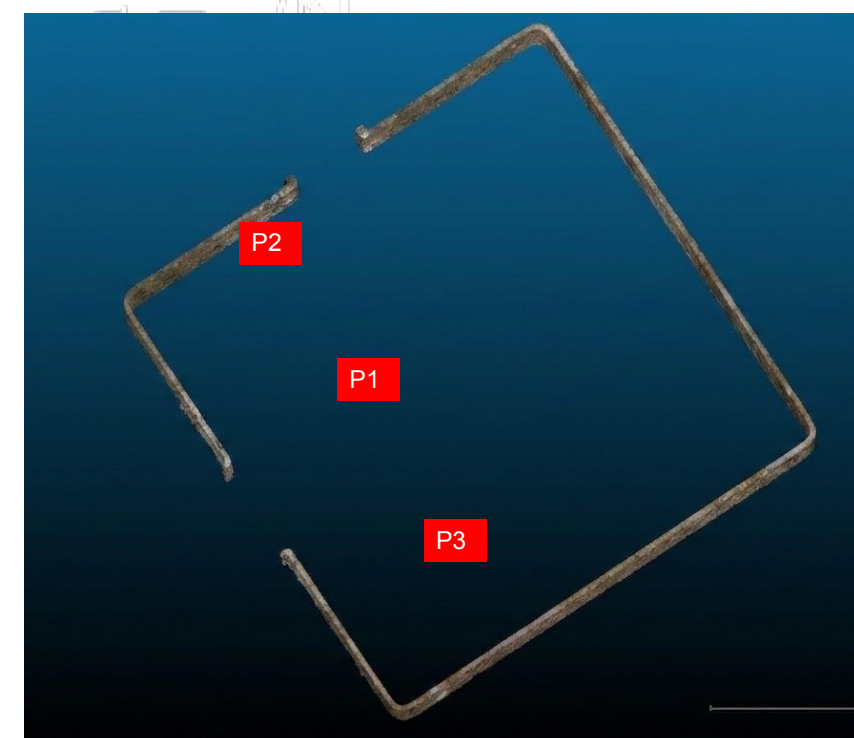
minimizing

Raw Data: Muon Counts Ground Floor

$p=1009.97$ hPa

$T= 20$ °C

Location	Slot 1 (600s)	Slot 2 (600s)	Slot 3 (600s)	Slot 4 (600s)	Average values	Total counts
P1 (Arch center)	46	46	37	43	43	126 ± 11.2
P2 (Right Side)	38	48	33	47	42	128 ± 11.3
P3 (Left Side)	38	38	52	46	44	136 ± 11.7



| Data Analysis & Equivalent Thickness

The fundamental principle of cosmic ray muon radiography (muography) relies on measuring the survival rate of muons as they propagate through matter. When a flux of atmospheric muons penetrates a solid structure, its intensity decreases due to continuous energy loss and scattering processes resulting from interactions with the atoms of the medium.

For civil engineering and shallow geological structures (up to several meters of rock or masonry equivalent), the reduction of the muon flux can be accurately modeled using a classic **linear-exponential attenuation law**:

$$R_i = e^{-x/\lambda}$$

where:

$$R_i = \frac{N_b/T_b}{N_{gnd}/T_{gnd}}$$

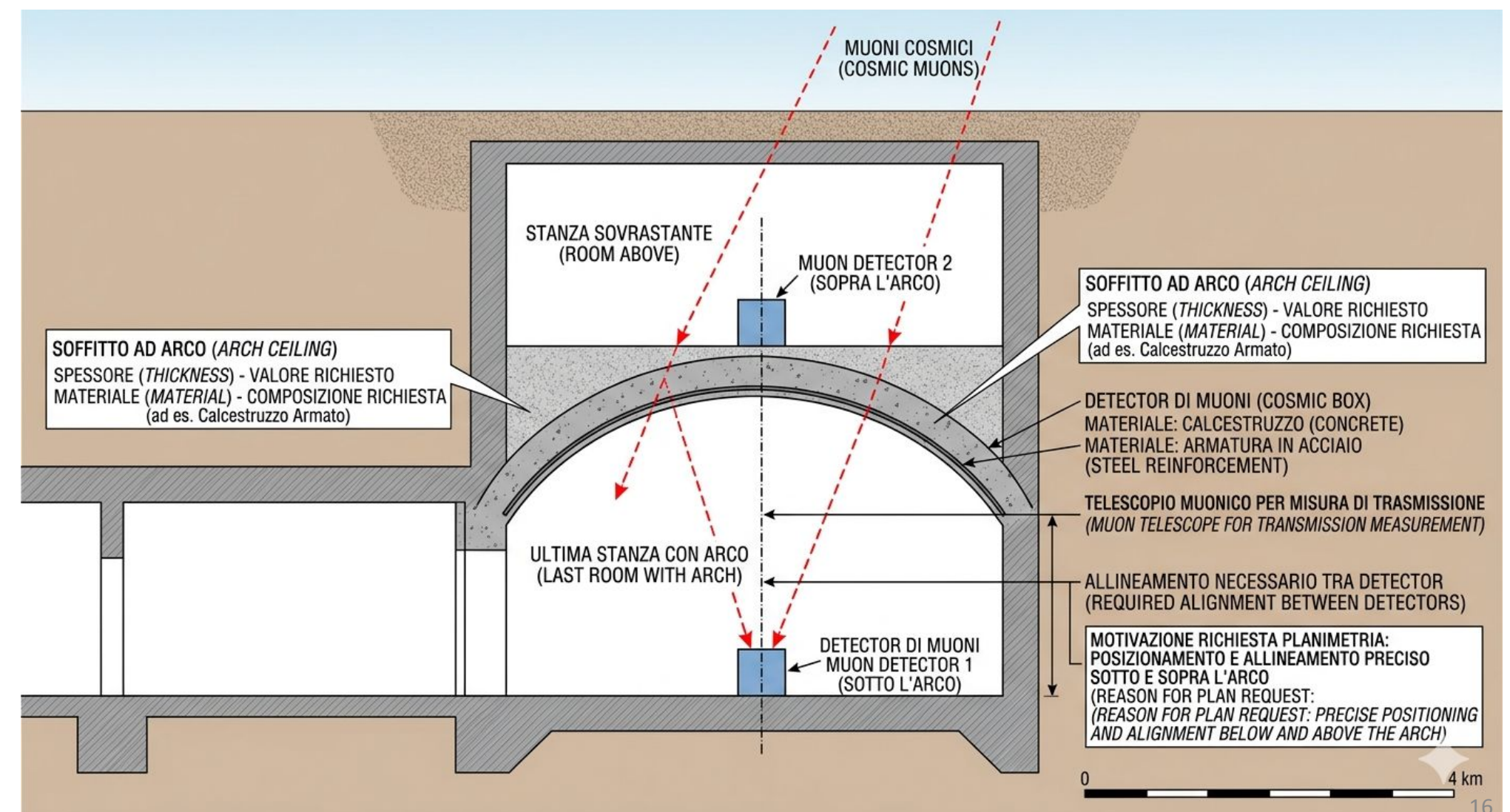
- **R_i** represents the **transmission ratio** defined as the ratio between the muon count rate per unit of time measured inside the bunker (N_b/t_b) and the muon count rate per unit of time recorded on the ground floor (N_{gnd}/t_{gnd})
- **x** is the **equivalent thickness** traveled by the particles through the material (expressed in meters or centimeters).
- **λ** is the **attenuation length** characteristic of the material under investigation (e.g., concrete or tuff).

- The **attenuation length for tuff** ($\lambda = 10.0$ m) adopted in the linear-exponential model is not an empirical parameter.
- It is directly derived from the ratio between the mean energy of the secondary muon spectrum at sea level (≈ 2.8 GeV) and the estimated linear stopping power of the medium ($dE/dx \approx 2.8$ MeV/cm).
- This stopping power was calculated based on the characteristic **density of compact tuff** ($\rho \approx 1.6$ g/cm³) combined with the **Minimum Ionization Loss** (MIP) coefficients officially tabulated by the Particle Data Group for standard rock and geological materials (≈ 1.75 MeV cm²/g).

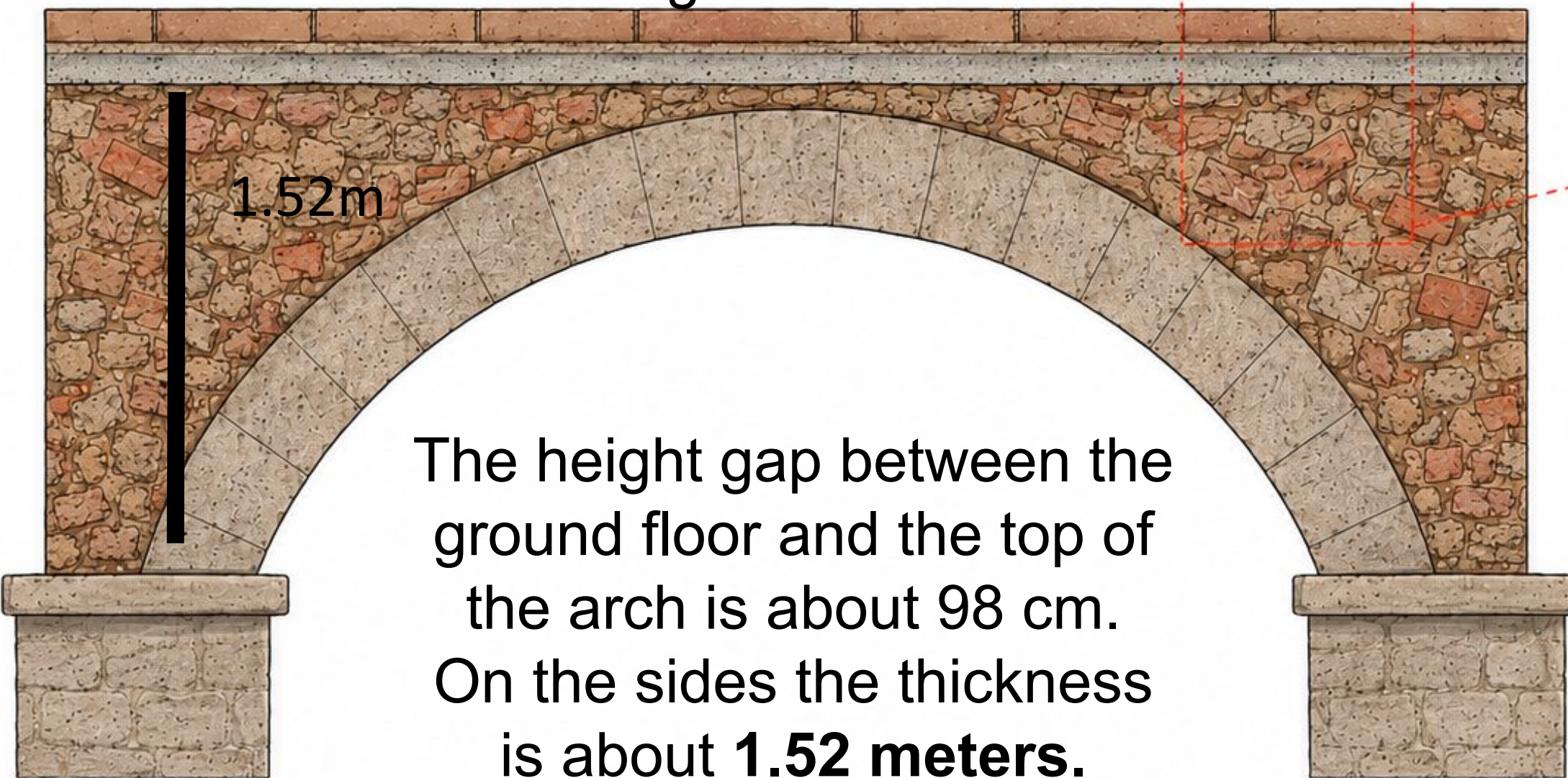
$$\frac{dE}{dx} = \text{MIP} \times \rho \qquad \lambda = \frac{E_{mean}}{\langle \frac{dE}{dx} \rangle}$$

- By multiplying this value by the characteristic density of compact tuff, we obtain the **linear stopping power** (≈ 2.8 MeV/cm)

- Finally, dividing the mean energy of the atmospheric muon spectrum (≈ 2800 MeV) by this linear stopping power yields an attenuation length (λ) of 10.0 m, which corresponds to the value used in the exponential absorption model.



ground floor



1.52m

The height gap between the ground floor and the top of the arch is about 98 cm. On the sides the thickness is about **1.52 meters**.



P3

P1

P2



Tuff masonry
(plastered)



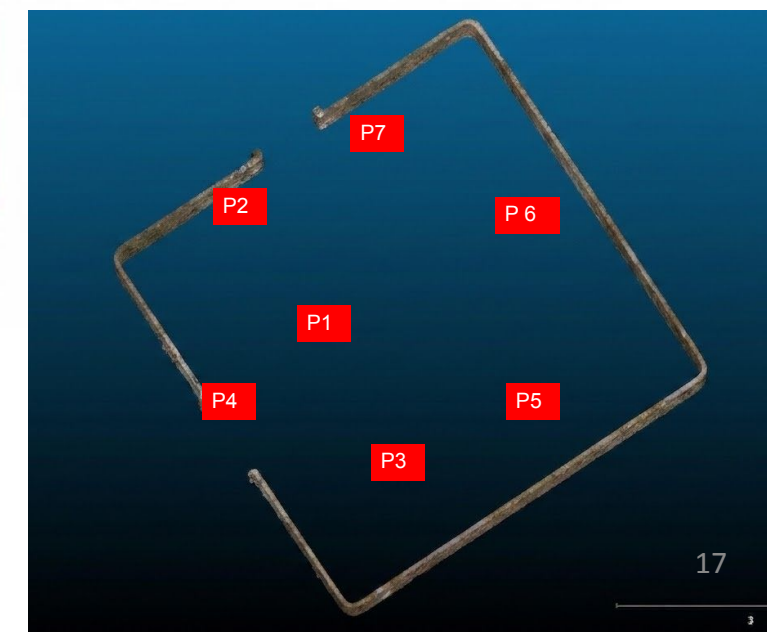
Backfill material
(bricks and tuff fragments)



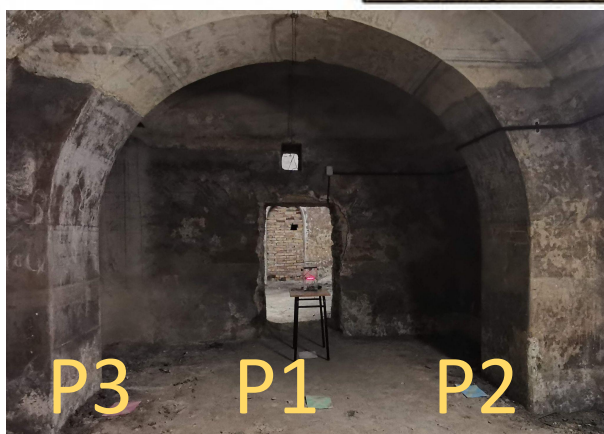
Thin screed
(lime or light cement)



Floor above



This results in a total traversed thickness of about **1.5–1.7 m**. medium likely consists of a composite stratigraphy, including **concrete** (foundations), **marble** (modern flooring), and **tuff** (the original structure of the bunker).



P3 P1 P2

Traversed thickness calculation with *average values*

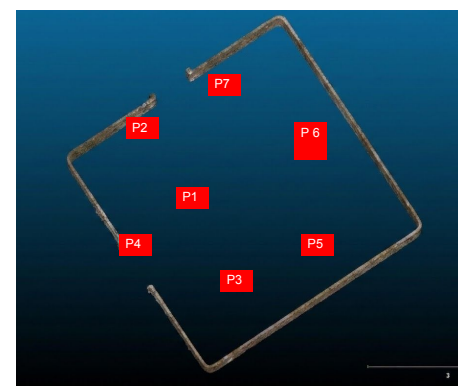
Location	Rbasement	Rgroundfloor	Ri	Xeq concrete (m)	Delta Thickness concrete (m)	Xeq tuff (m)	Delta Thickness tuff (m)
P1 (Arch center)	46	43	1,07	-0,45	1,97	-0,67	2,19
P2 (Right Side)	34	41,5	0,82	1,33	0,19	1,99	-0,47
P3 (Left Side)	37	43,5	0,85	1,08	0,44	1,62	-0,10

$$\Delta tks = 1,52m - Xeq$$

If $\Delta tks > 0 \implies Deficit$

If $\Delta tks < 0 \implies Surplus$

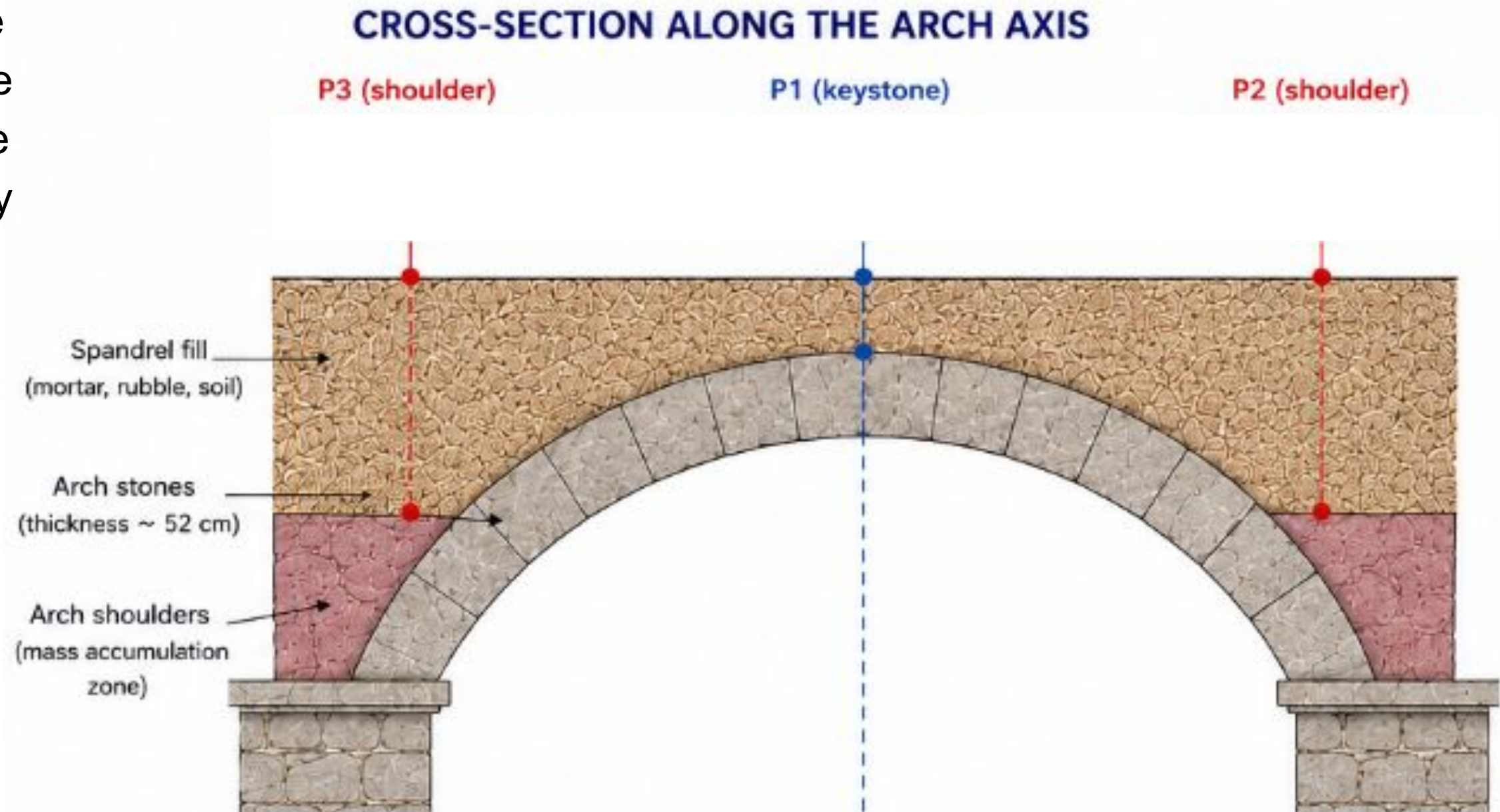
Results and Discussion



- **Other Points (P4, P5, P6 and P7):** Muon counts at ground and basement levels are nearly identical ($=46$ or >40), proving the vault's shielding is **negligible** compared to overlying school building.

- **Central Zone (P1):** Thickness values are near zero or slightly negative, confirming the **vault crown** as the thinnest section, where the bunker ceiling and school floor nearly meet.

- **Right Side (P2):** Shows the largest delta (-0.47), reflecting **structural complexity** and also due to their angular distribution (acceptance cone).

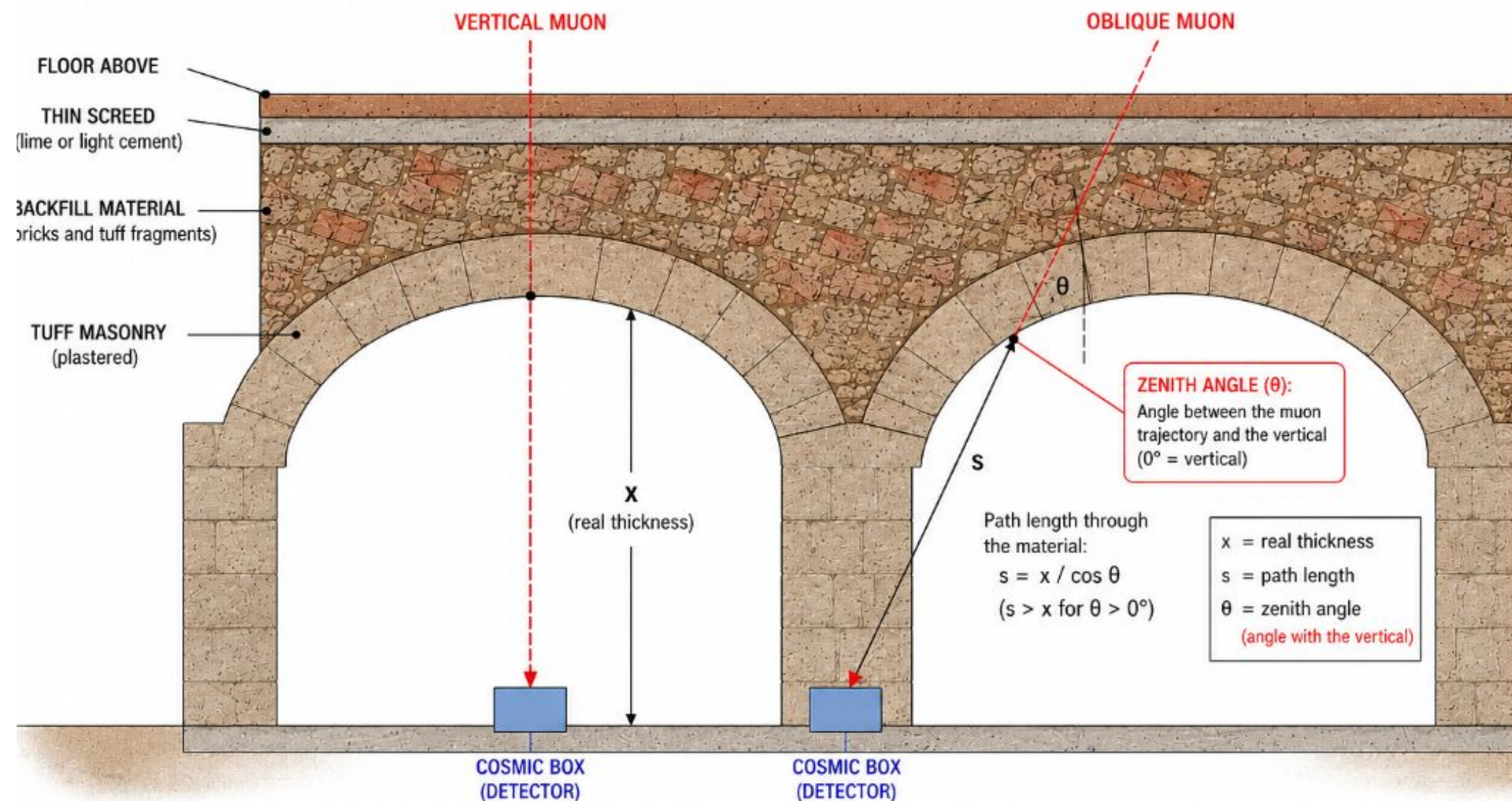


Results and Discussion

Right Side (P2)

The measured mass surplus or deficit is not due to high-density materials but to the **geometry of the shared wall**:

- **Path Length Effect:** Muons on slanted (non-vertical) trajectories travel a longer physical distance through the stone, increasing perceived density.
- **Shared Piedritto:** The detector measures the combined mass of the **52-cm vault ceiling** and the **95-cm stone core** of the shared load-bearing wall.



$$s = \frac{x}{\cos \theta}$$

Left Side (P3)

It has the smallest delta in absolute terms **(-0,10)**. This rules out that the entire spandrel area is confirmed to be completely solid and compact, backfilled with high-density stone fragments and lime mortar.

Thank to

- Prof. Nicola Scardigno - Dipartimento di Architettura Politecnico di Bari
- Prof. Alessandro Crispino - Liceo Scientifico “Scacchi”- Bari
- Prof. Luigi Riviello - Liceo Scientifico “Scacchi”- Bari

Thank you for the attention

References

- Groom, Mokhov, Striganov, PDG, Muon stopping power and range tables, Atomic Data and Nuclear Data Tables, Vol. 76, No. 2, July 2001
- Lesparre et al., Geophysical muon imaging: feasibility and limits, Geophys. J. Int., 2010.
- Braucher et al., Determination of muon attenuation lengths, EPSL, 2013.
- Cecchini & Spurio, Atmospheric muons: experimental aspects, Geosci. Instrum. Meth., 2012.
- Nagamine K., Introduction to Muon Radiography, 2016.
- Saracino et al., Imaging of underground cavities with cosmic-ray muons from observations at Mt. Echia (Naples), Scientific Reports volume 7 (2017)
- G. Saracino et al., Applications of muon absorption radiography to the fields of volcanology and civil engineering —Physics of the Earth and Planetary Interiors (2018) / pubblicato su PMC.

